Experimental Investigations of Backward Transition Radiation Characteristics in Extreme Ultraviolet Region

A.P. Potylitsyn[(1)], D. Krambrich[(2)], G. Kube[(3)], W. Lauth[(2)], Yu.A. Popov[(1)], and L.G. Sukhikh[(1)]

1 - Institute of Physics and Technology, Tomsk Polytechnic University, Tomsk, Russia

2 - Institut fur KernPhysik, Johannes Gutenberg University, Mainz, Germany

3 - Deutsches Elektronen-Synchrotron (DESY), Hamburg, Germany

Optical transition radiation (OTR) beam size monitor

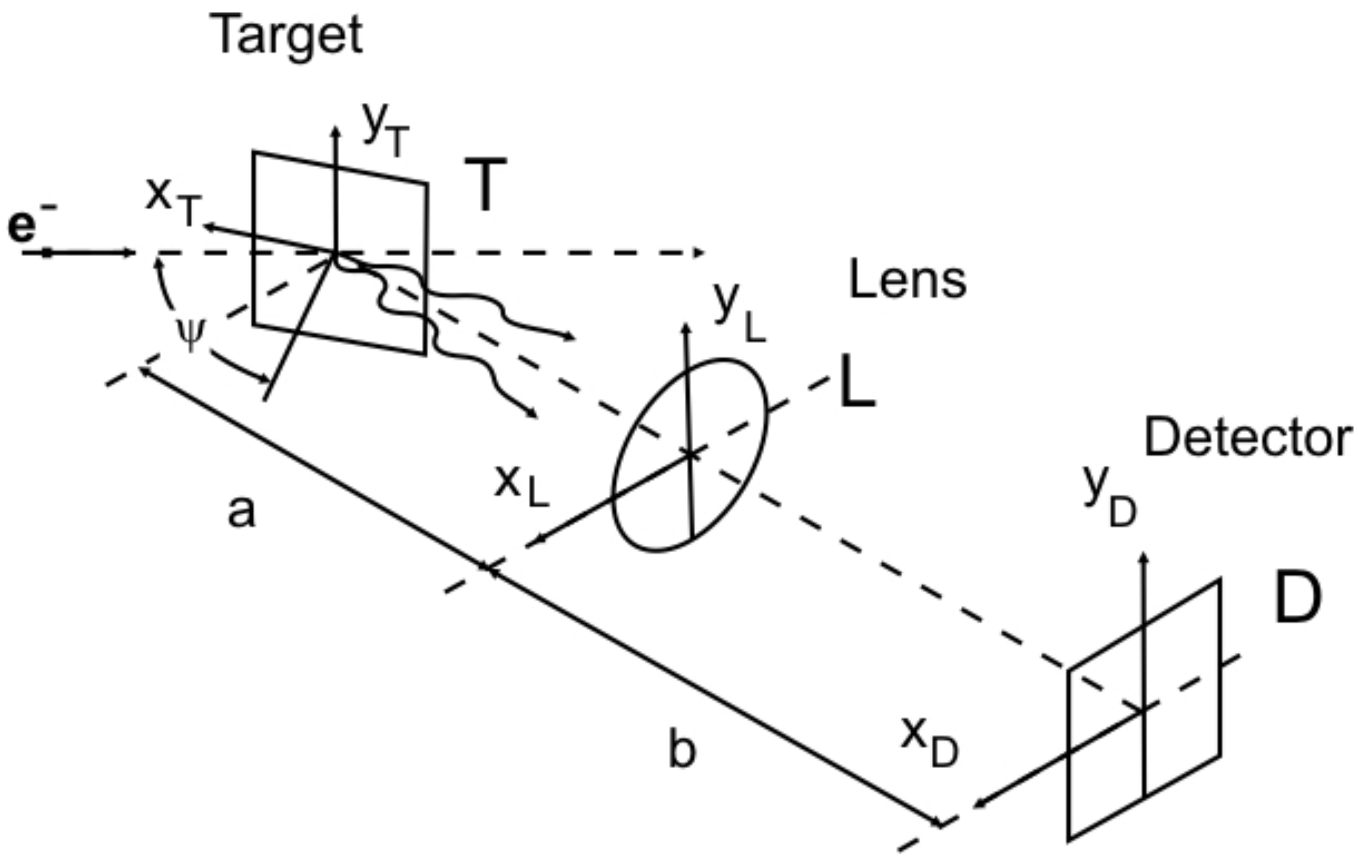

A Very High Resolution Optical Transition Radiation Beam Profile Monitor // **Ross M. et al.** SLAC-PUB-9280 July 2002

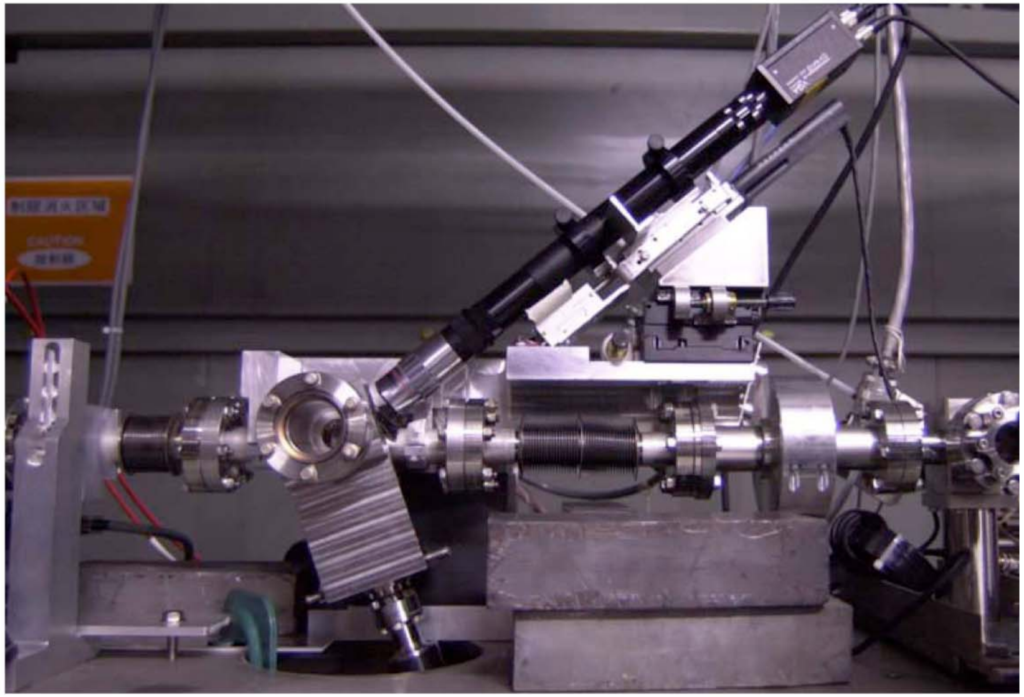

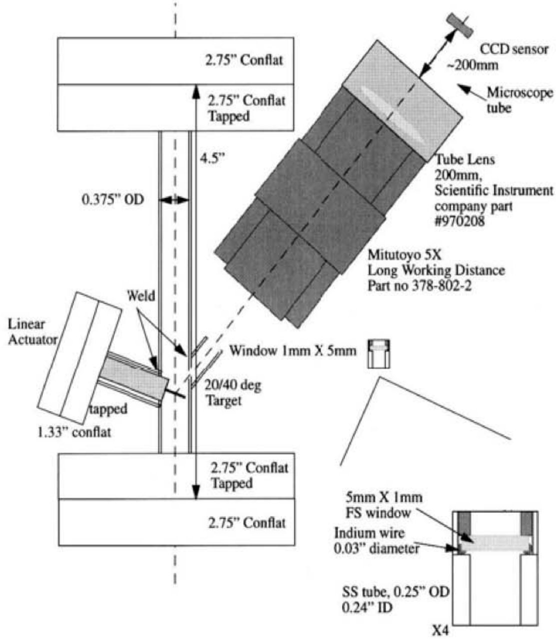

The OTR monitor was installed in the KEK-ATF extraction line.

A Very High Resolution Optical Transition Radiation Beam Profile Monitor // Ross M. et al. SLAC-PUB-9280 July 2002

Optical wavelengths
λ~550 nm

σ = 2 μm

$FWHM = 10\mu$

$FWHM = 5.8\mu$

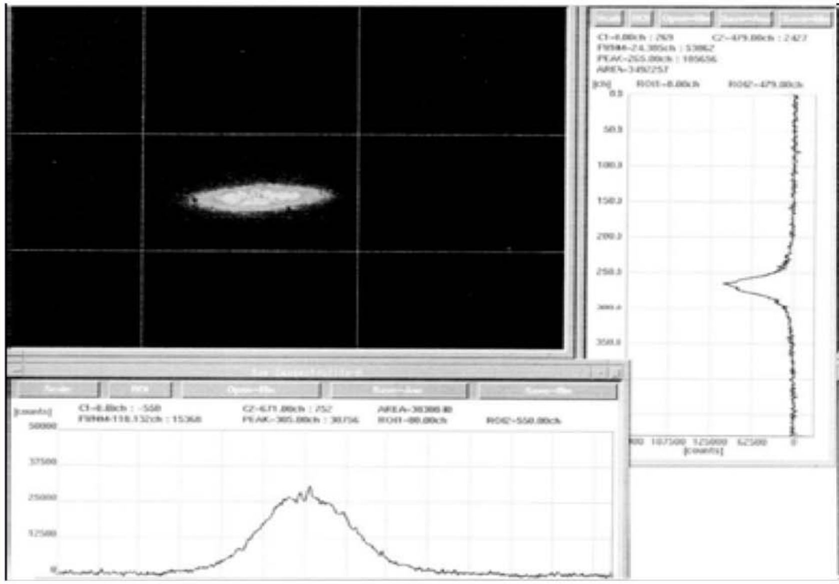

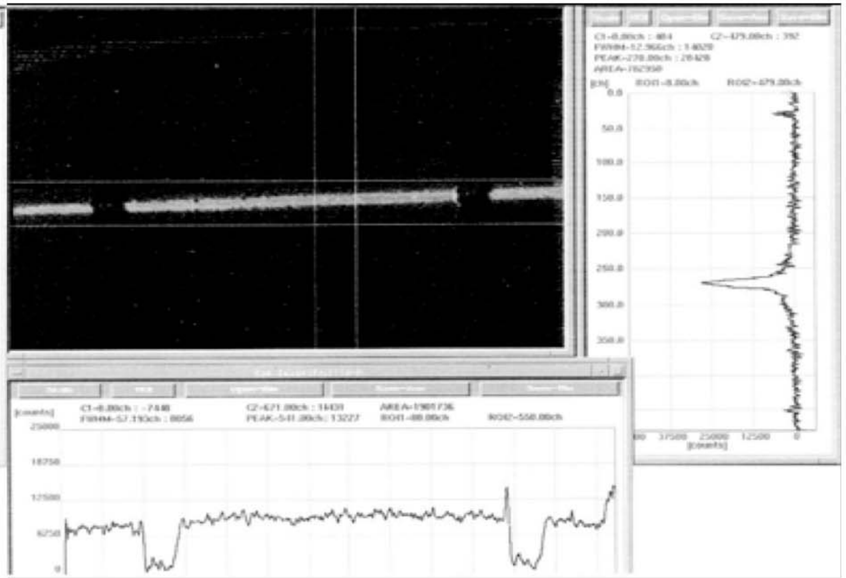

Coherent OTR

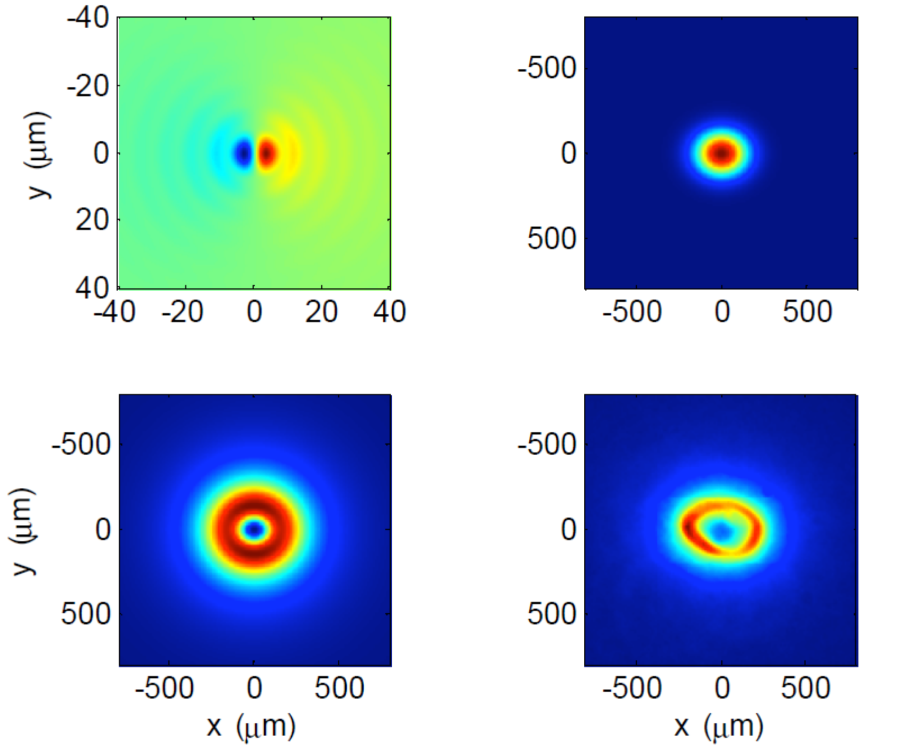

Figure 7: Simulation of COTR image. Upper panel left is the horizontal component of the source field, right is the beam distribution, lower panel left is the simulated COTR image and right the measured image.

H. Loos et al., OBSERVATION OF COHERENT OPTICAL TRANSITION RADIATION IN THE LCLS LINAC, SLAC-PUB-13395, (2008)

Coherent OTR

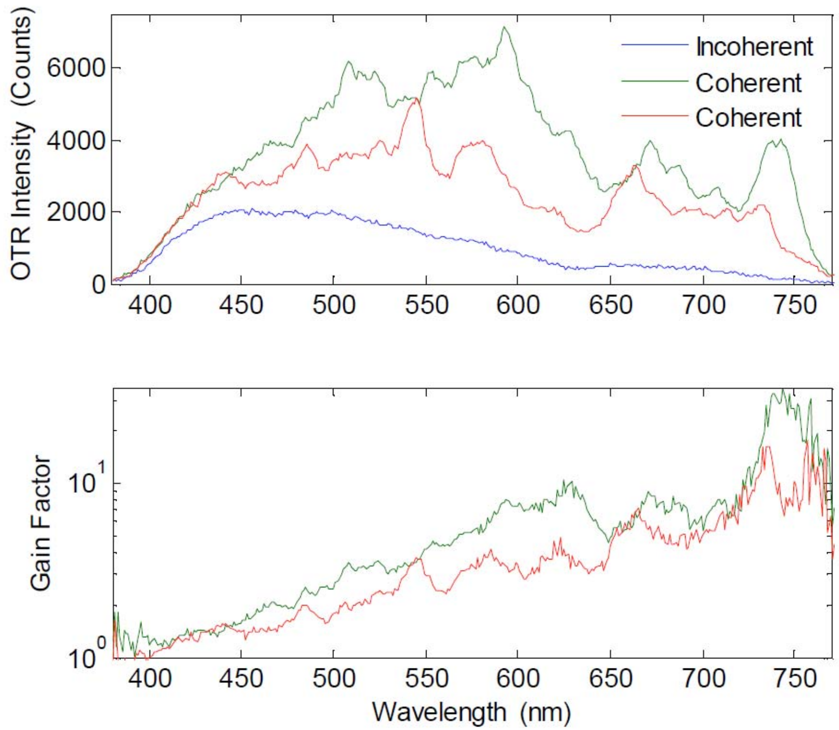

Figure 6: OTR light spectra after BC1 with the beam under normal compression (red and green) and with the coherence suppressed (blue). The spectra are in the upper panel and the spectral gain factor (ratio of coherent to incoherent spectrum) in the lower one.

H. Loos et al., OBSERVATION OF COHERENT OPTICAL TRANSITION RADIATION IN THE LCLS LINAC, SLAC-PUB-13395, (2008)

Resume

- There may be serious problems using the beam diagnostics based on OTR at X-FELs.
- There is almost no possibility to use the beam diagnostics based on OTR at colliders with small transverse beam sizes.
- We need simple and reliable tool for beam transverse size measurement in the cases when optical TR does not work:
  - Small beam sizes (sub-micron)
  - Coherent radiation
- We propose to use TR in Extreme Ultraviolet Range (EUV TR) for these purposes

Some theory

In our theoretical estimations we will follow the a simple method of transition radiation generation in an ideally reflecting target. The real optical properties of the target may be taken into account using the Fresnel reflection coefficients. In this case the radiation field may be written using projection angles θ_x and θ_y that are counted from the specular reflection direction

$$\boxed{\begin{gathered}\mathbf{E}(\theta_x, \theta_x) = \frac{e\beta}{\pi c} \frac{1}{\beta^2 \cos^2\theta_x \cos^2\theta_y - 1} \frac{e^{i\mathbf{kr}}}{r} \\ \{-\cos\theta_x \sin\theta_x \cos\theta_y, -\cos^2\theta_x \cos\theta_y \sin\theta_y, \\ \sin^2\theta_x + \cos^2\theta_x \sin^2\theta_y\} \qquad (1)\end{gathered}}$$

Here e is the electron charge, β is the speed of particle in the speed of light units, c is the speed of light, $\mathbf{k}$ is the wave-vector, $\mathbf{r}$ is the detector coordinate. The spectral-angular density of the radiation taking into account the Fresnel reflection coefficients R_σ and R_π:

$$\boxed{\frac{d^2W}{\hbar d\omega d\Omega} = \frac{cr^2}{\hbar} \left[|R_\sigma E_y|^2 + + |R_\pi|^2 \left(|E_x|^2 + |E_z|^2 \right) \right] \quad (2)}$$

In other words backward transition radiation is treated as a reflection of the virtual photon flux connected with an initial charged particle by a target, which may be considered as a specific mirror.

Mainz Microtron MAMI-B

EXPERIMENTAL PART

Experimental layout

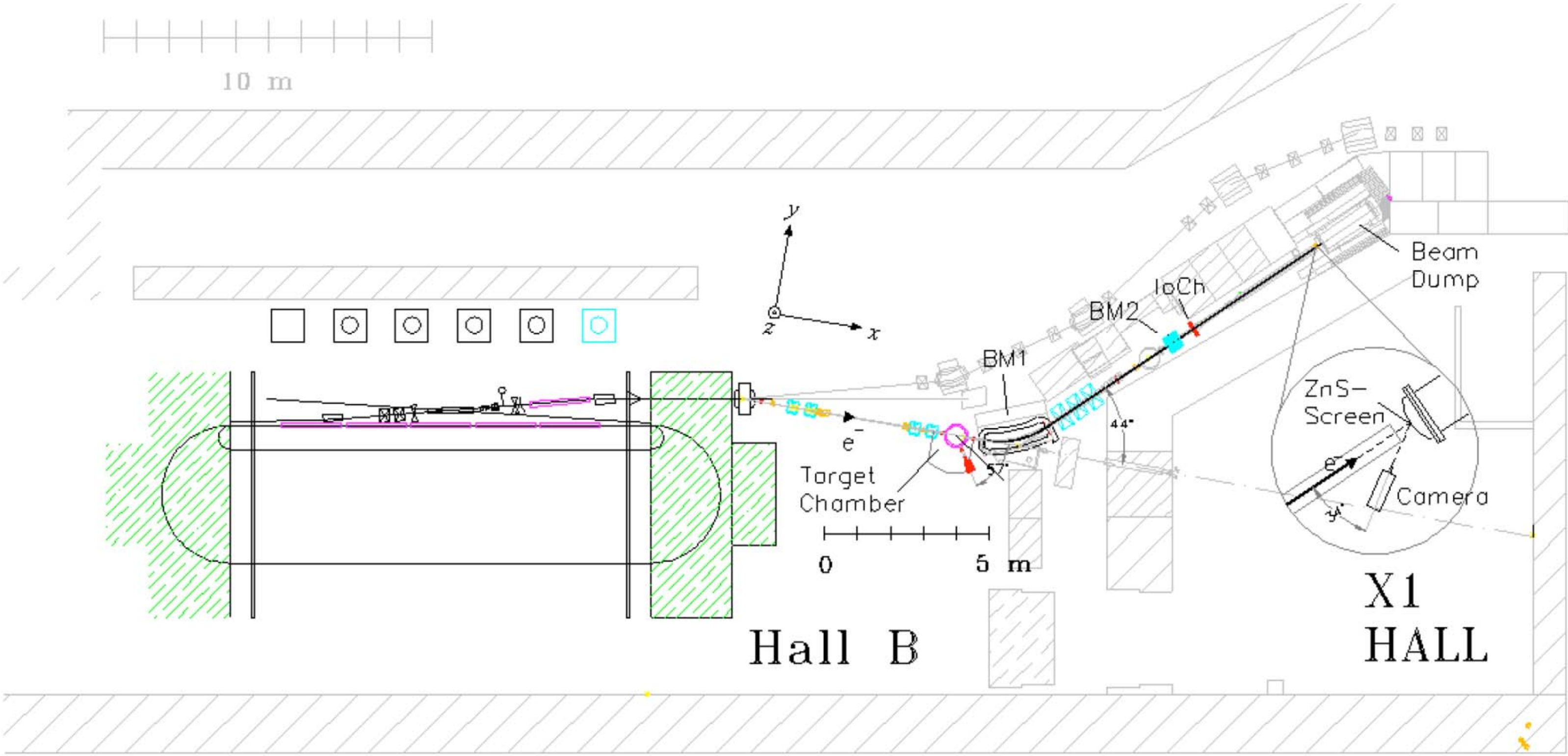

Electron energy – 855 MeV

Experimental layout

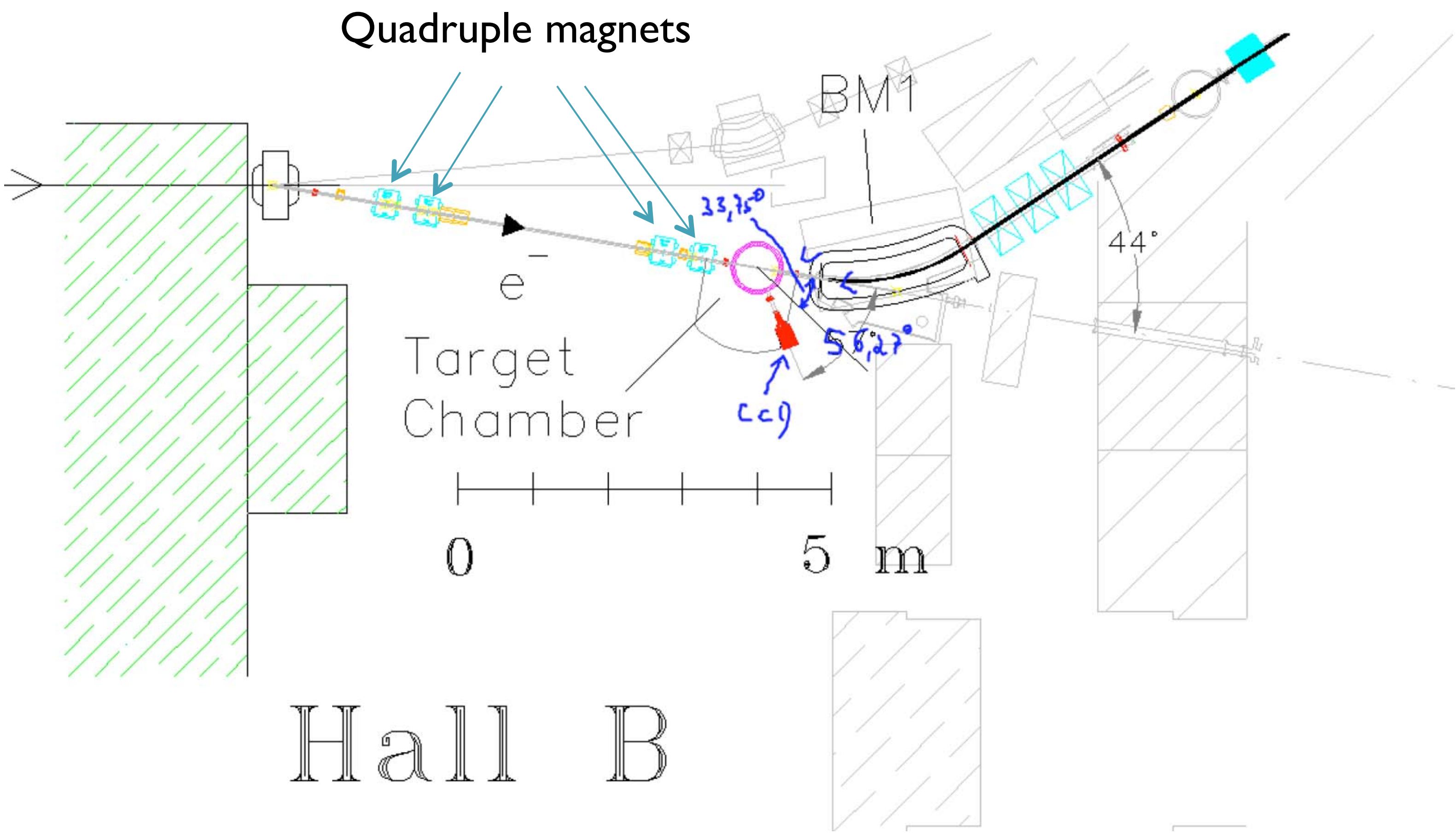

Experimental setup

- MAMI electron beam with electron energy 855 MeV, with average beam current 52 nA was used. The beam was bunched (so-called ``diagnostic pulse mode'') with bunch duration 0.8 sec and period 3 sec. The beam interacted with a target that was setup on the goniometer. The target was molybdenum layer (500 nm) which was chosen due to high reflectivity in EUV region with surface roughness better than 1 nm evaporated on a silicon substrate with thickness equal to 500um.
- The target dimensions were 40*10 mm^2. During the experiment the target was setup at two grazing angles: alpha=28.075 deg (so-called ``forward'' direction) and alpha=67.5 deg (so-called ``backward'' direction).
- During the experiment different beam configurations were used

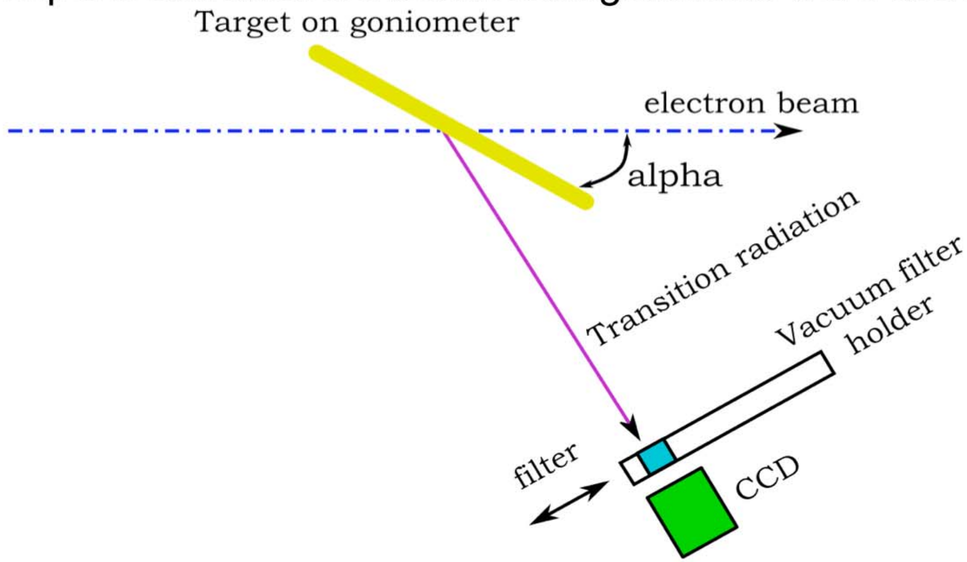

Experimental setup

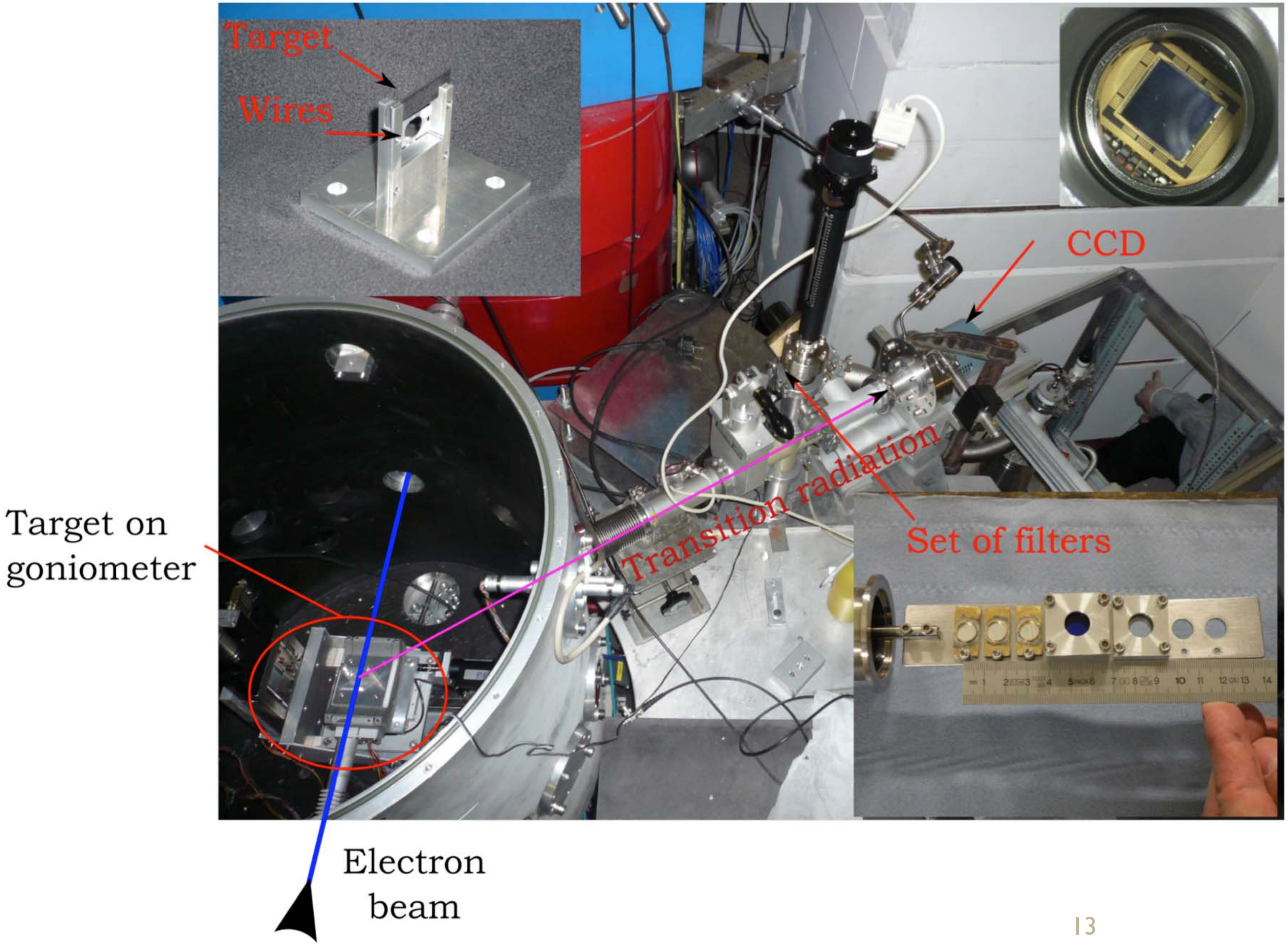

Beam configurations

TABLE I: Beam sizes in the interaction point

No.	Vert. FWHM, μm	Horiz. FWHM, μm
1	64.3	533
2	542	365
3	247	6111

CCD camera and filters

TABLE II: Filter characteristics

No.	Type
1	Aluminum foil 1.3 μm (2 layers of 0.65 μm)
2	Aluminum foil 1.8 μm
3	Fused silica with 3 mm thickness
4	Blue bandpass optical filter BG-12, $\Delta\omega/\omega = 0.35$

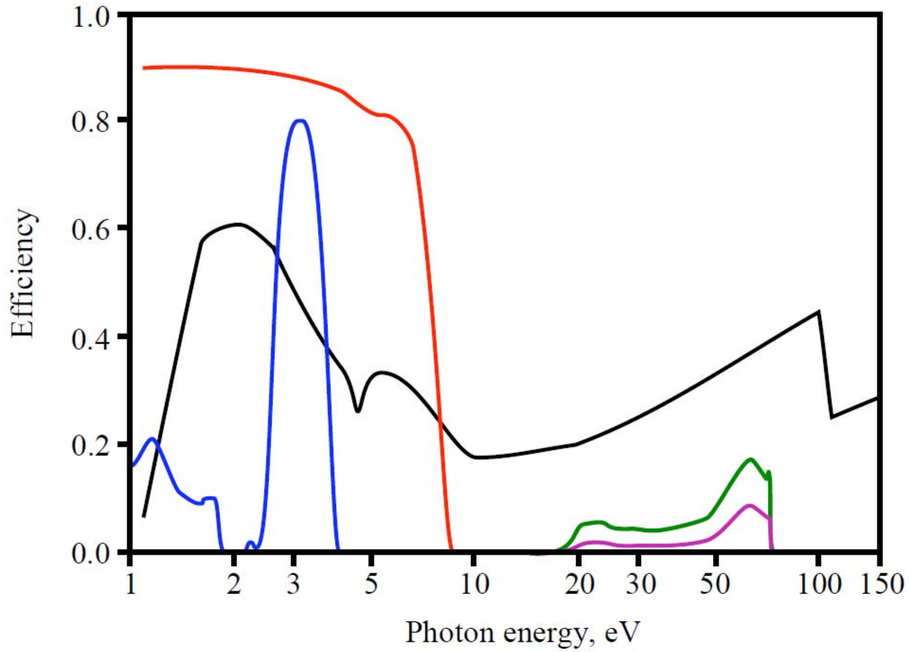

FIG. 2: Transmission coefficients of the filters and CCD quantum efficiency (black curve). Filter No. 1 – green curve, No. 2 – pink curve, No. 3 – red curve, No. 4 – blue curve.

Andor DO-434 BN
1024 x 1024 pixel
pixel size 13μmx13μm

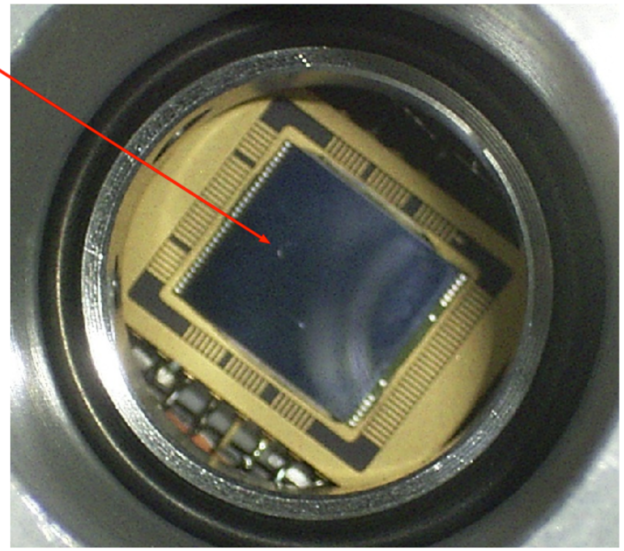

Fused silica filter 28.07 deg

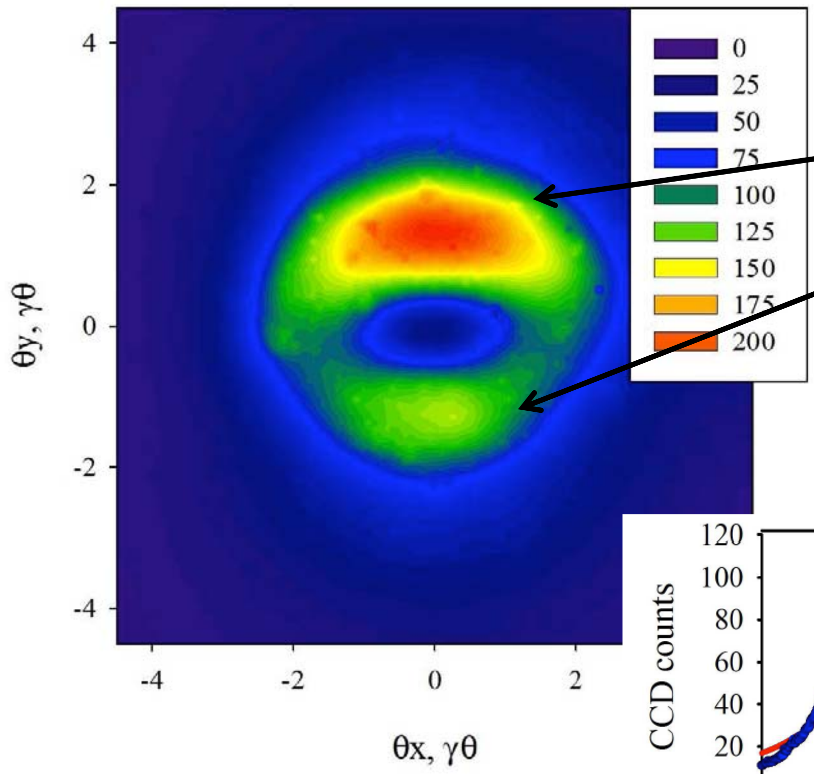

Asymmetry?

FIG. 3: The spatial distribution of backwa
radiation obtained with the filter No.3.

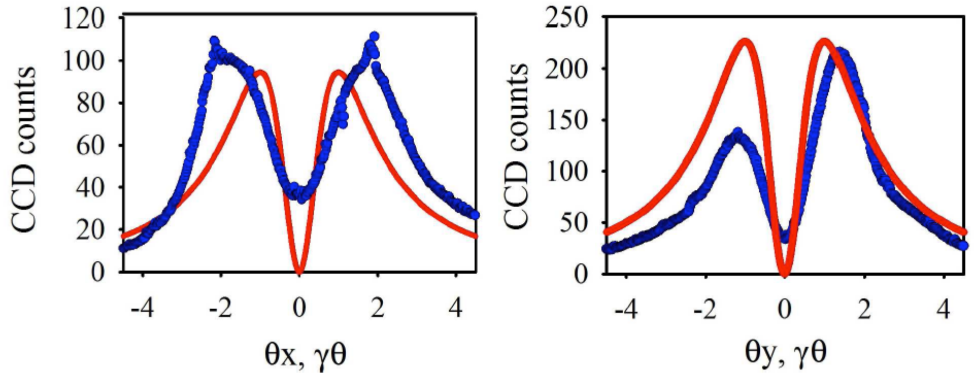

FIG. 4: Cross sections along x and y directions obtained with the filter No.3 (blue dots). Theoretically predicted distributions are shown by the red line and divided by 2.

Asymmetry reason - QUAD radiation?

67.5 deg, beam No. 1
(All QUADs are on)

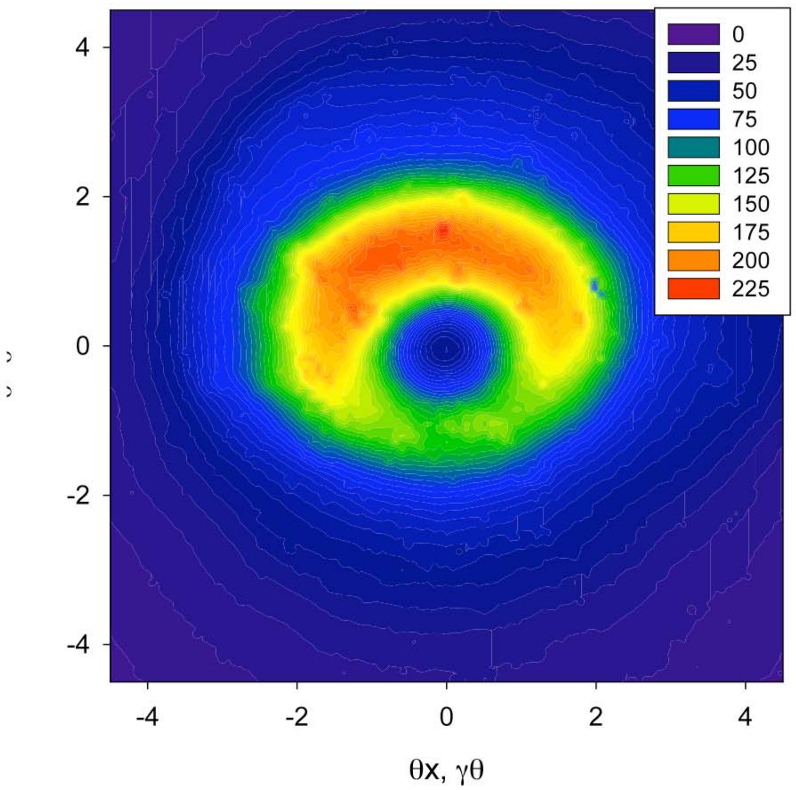

67.5 deg, beam No. 3
(QUADs are off)

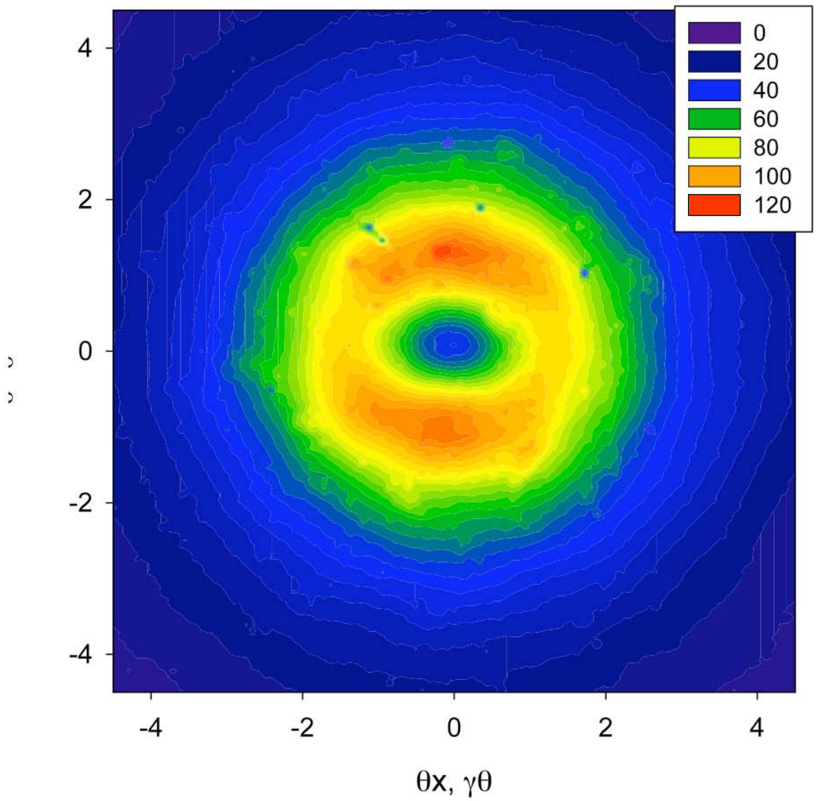

Fused silica filter

TABLE III: Characteristics of optical transition radiation for different beam shapes obtained with the filter No. 3.

Beam	α, deg	Inter-peak distance, γ^{-1}	Asym., %	Total, 10^6 CCD counts
No.1	28.07	x: 3.7 y: 2.6	x: 0.6 y: 23	8.85
	67.5	x: 3 y: 2.6	x: 3.3 y: 26.8	10
No.2	28.07	x: 2.3 y: 2.6	x: 2.8 y: 9.5	7.14
	67.5	x: 2.4 y: 2.7	x: 6.3 y: 9.3	7.45
No.3	67.5	x: 2.8 y: 2.4	x: 0.9 y: 1.1	6.92

Small difference

Theory

28.07 deg - $2*10^7$ counts

67.5 deg $2.1*10^7$ counts

Bandpass blue filter 28.07 deg

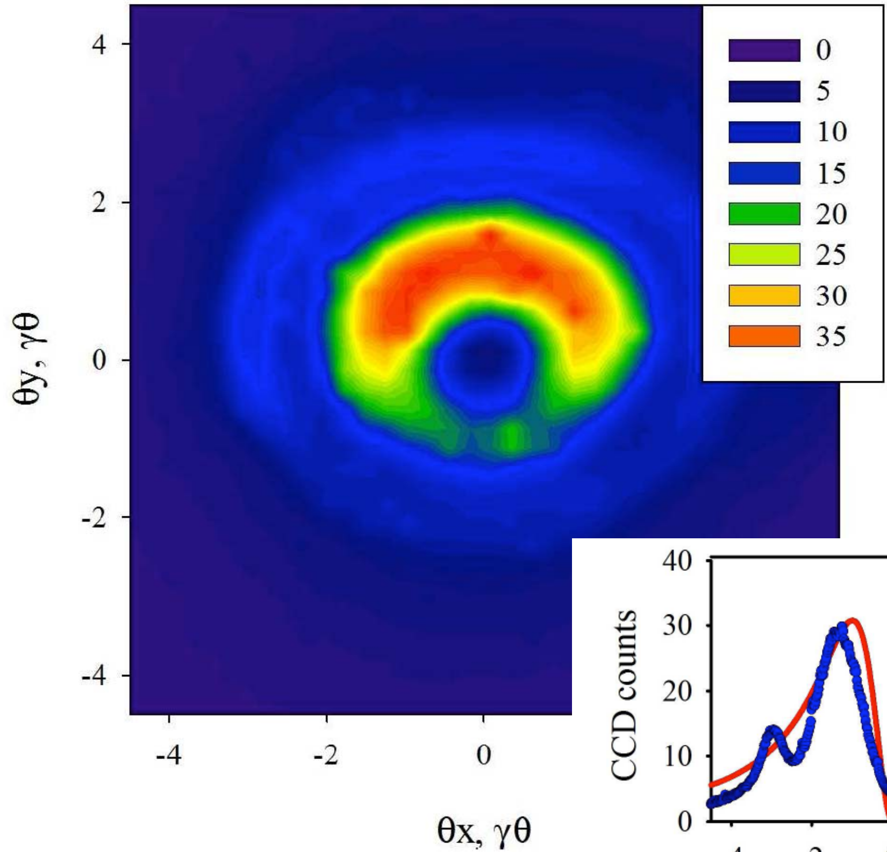

FIG. 5: The spatial distribution of
radiation obtained with the filter N

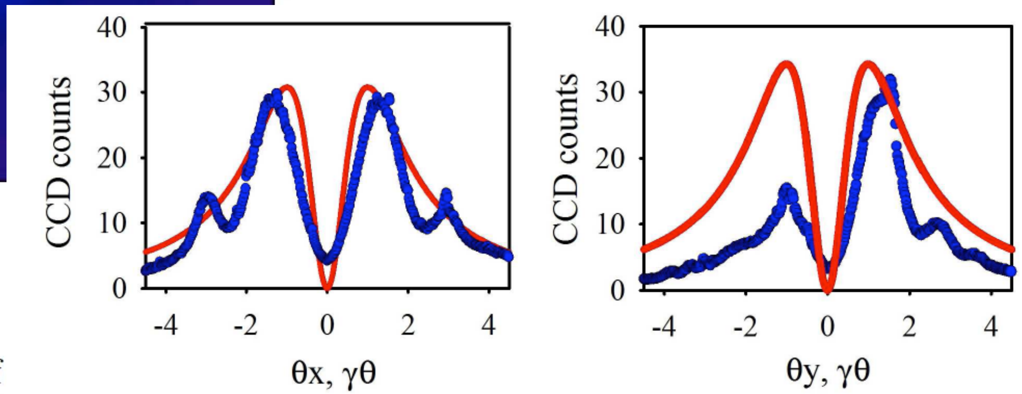

FIG. 6: Cross sections along x and y directions obtained with the filter No.4 (blue dots). Theoretically predicted distributions are shown by the red line and divided by 2.

Bandpass blue filter

TABLE IV: Characteristics of optical transition radiation for different beam shapes obtained with the filter No. 4

Beam	α, deg	Inter-peak distance, γ^{-1}	Asym., %	Total, 10^6 CCD counts
No.1	28.07	x: 3.1 y: 2.2	x: 1.8 y: 33	1.24
	67.5	x: 2.6 y: 2.3	x: 0.7 y: 36.5	1.44
No.2	28.07	x: 1.9 y: 2.4	x: 0.2 y: 14	1
	67.5	x: 2.1 y: 2.3	x: 11 y: 12	1
No.3	67.5	x: 2.7 y: 2.2	x: 5.7 y: 1.6	0.95

Small difference

Theory

28.07 deg - $3.98*10^6$ counts

67.5 deg $4.1*10^6$ counts

Al foil 1.3 um 28.07 deg

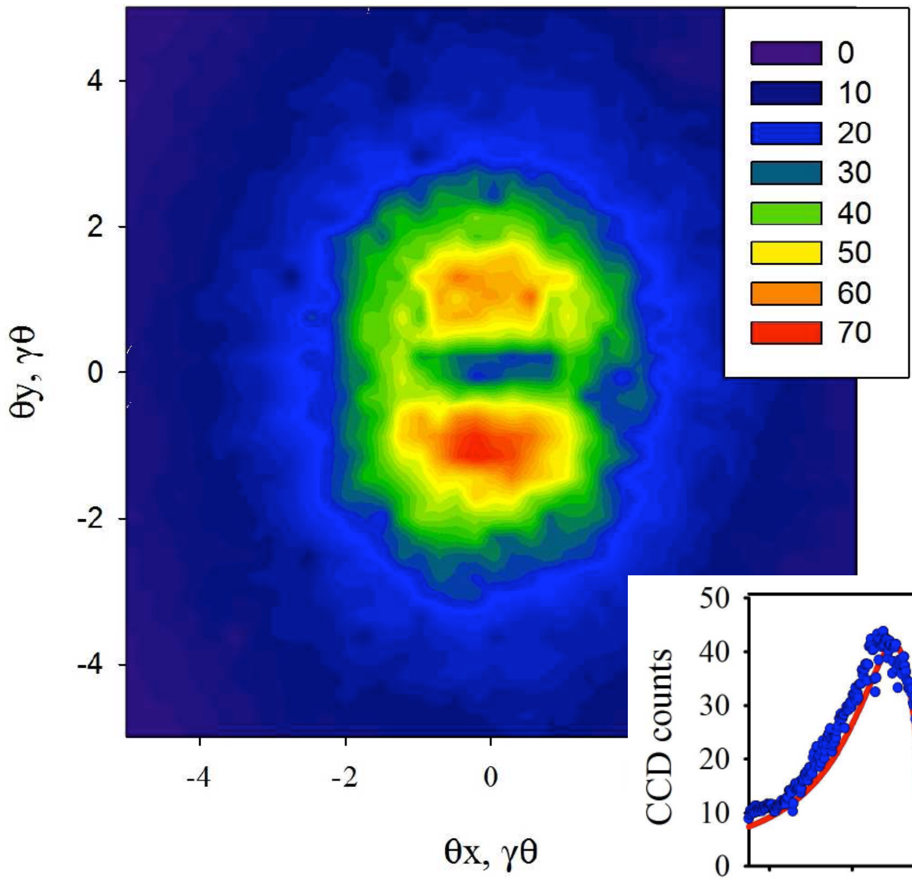

FIG. 7: The spatial distribution of ba
radiation obtained with the filter No.1

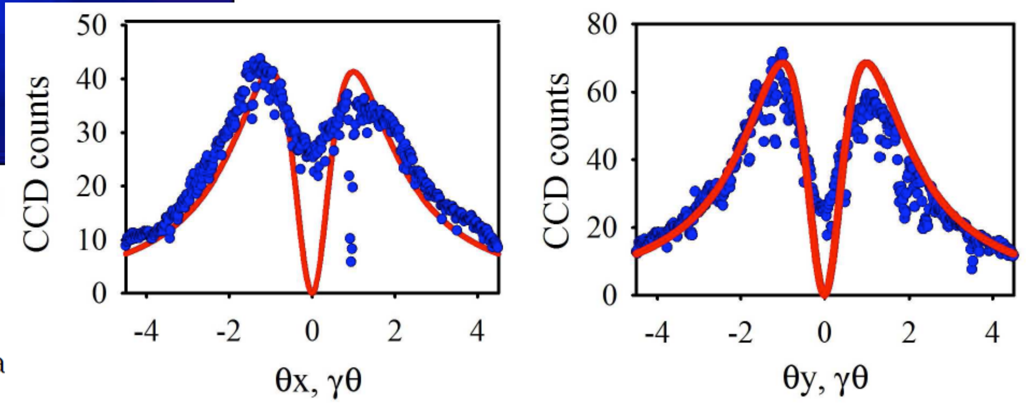

FIG. 8: Cross sections along x and y directions obtained with the filter No.1 (blue dots). Theoretically predicted distributions are shown by the red line and multiplied by 6.

Al foil 1.3 um

TABLE V: Characteristics of EUV transition radiation for different beam shapes obtained with the filter No. 1.

Beam	α, deg	Inter-peak distance, γ^{-1}	Asym., %	Total, 10^6 CCD counts
No.1	28.07	x: 2.3 y: 2.2	x: 8.3 y: 5	3.57
	67.5	x: 1.7 y: 2.1	x: 1.3 y: 3.3	0.45
No.2	28.07	x: 1.7 y: 2.2	x: 1.9 y: 5.9	2.44
	67.5	x: 1.4 y: 2.5	x: 0.7 y: 0.1	0.38
No.3	67.5	x: 2.1 y: 2.1	x: 2.9 y: 1.5	0.40

Large difference

Theory

28.07 deg - $5.8*10^5$ counts

67.5 deg - $0.6*10^5$ counts

Molybdenum reflection coefficients

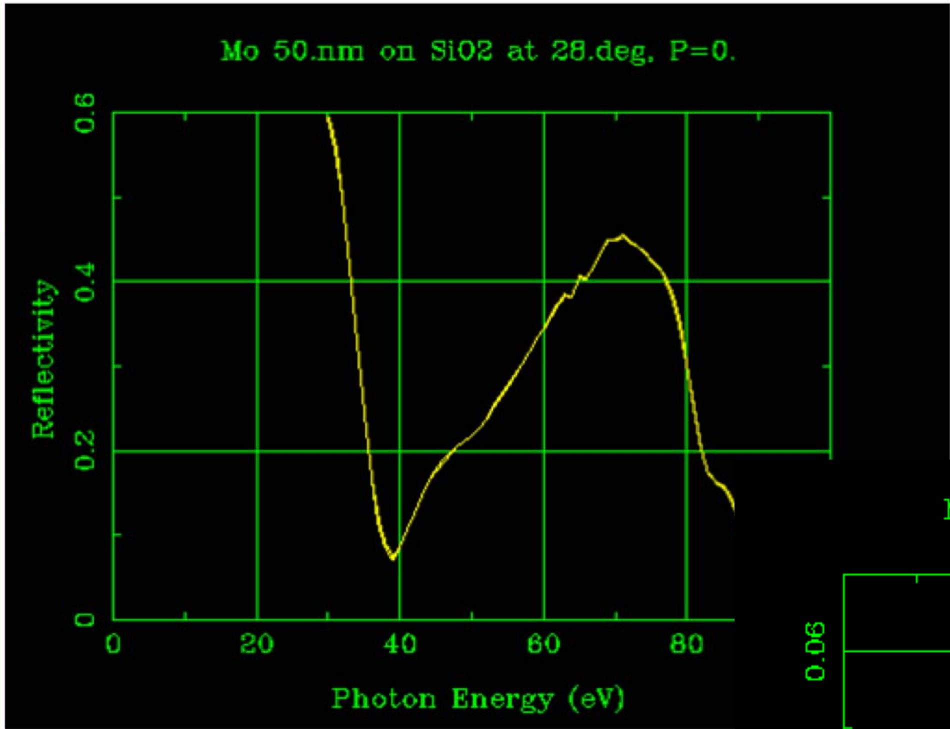

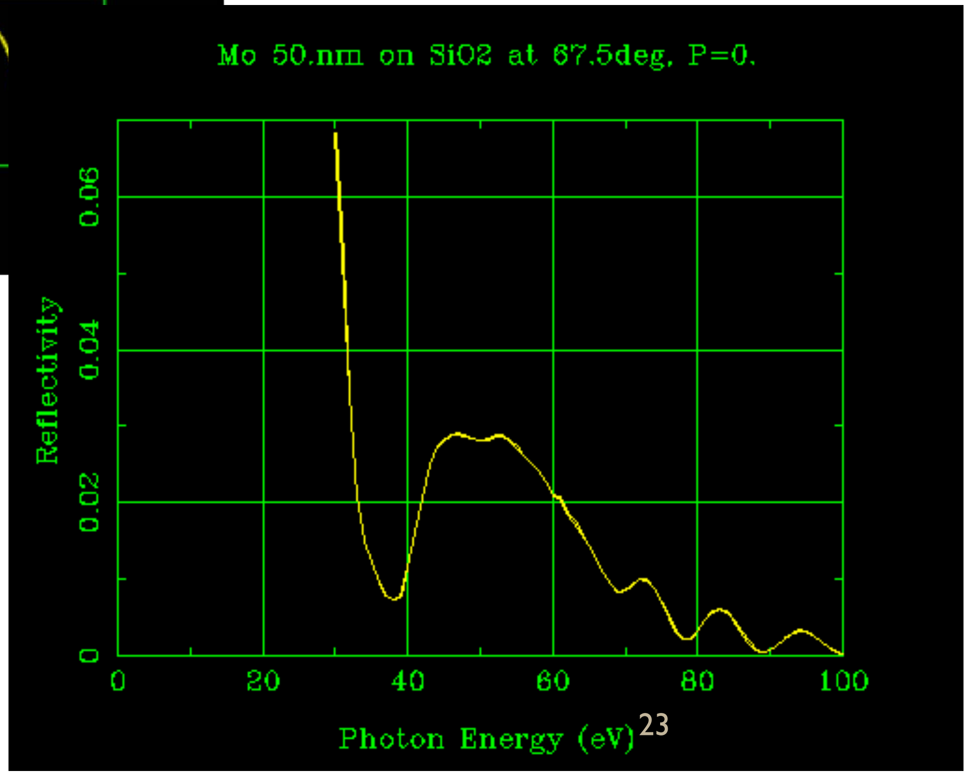

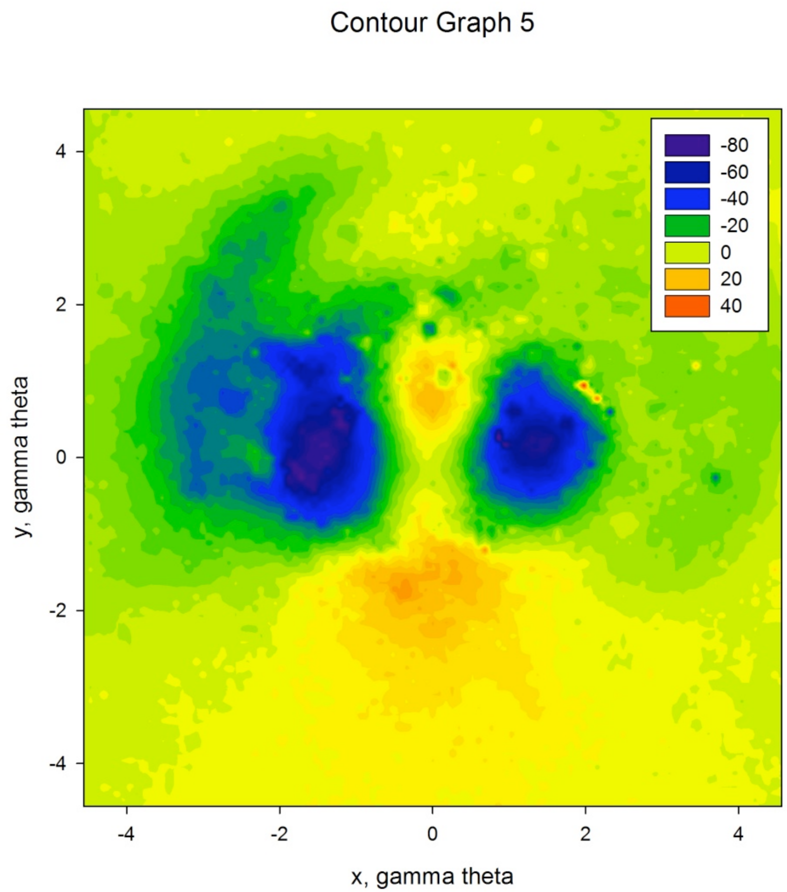

- The figure shows the difference of two measured distribution of radiation with Fused Silica filter in forward geometry – backward geometry. Beam configuration No. 3

- The difference shows that intensity of radiation is almost the same at different angles. The difference is caused by the difference of polarization components

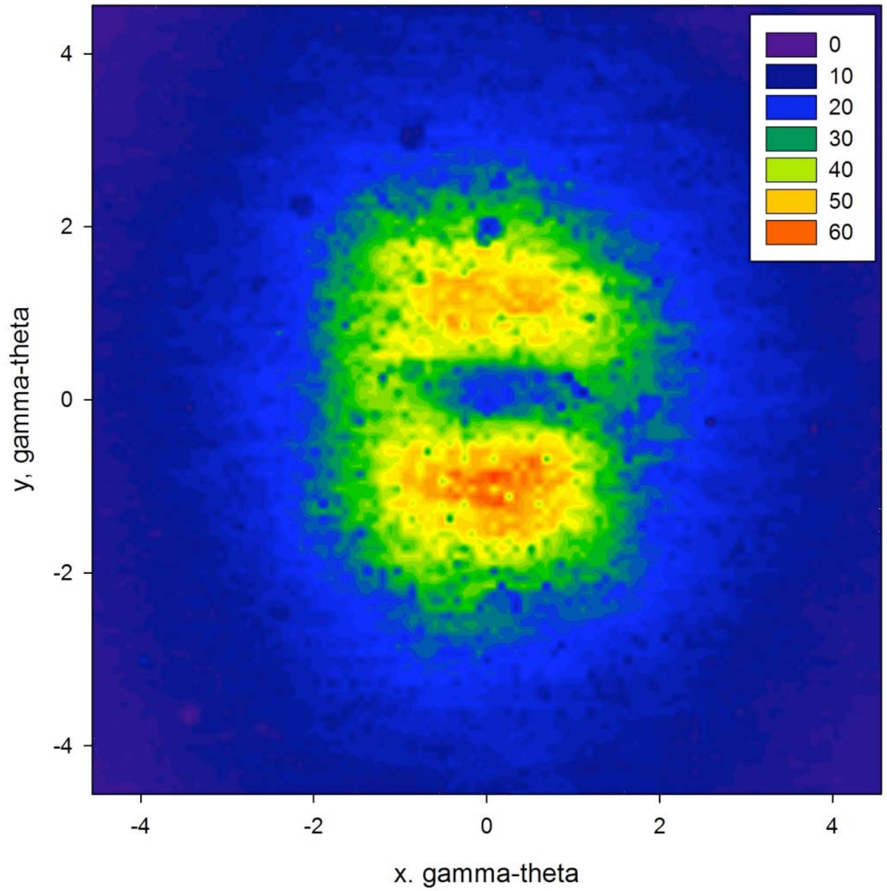

- The figure shows the difference of two measured distribution of radiation with Aluminum 1,3 micron filter in forward geometry – backward geometry. Beam configuration No. 3

- The difference shows that intensity of radiation is different at different angles. That proves the EUV character of radiation.

Conclusion

- Experimentally measured backward transition radiation in EUV region is rather powerful and was observed reproducibly
- The measured radiation in this region is more powerful than it was theoretically predicted
- The radiation measured in EUV region is more symmetrical and it seems that influence of parasitic synchrotron radiation is suppressed

Future plans

- As the next step we plan to install multilayer focusing mirror that makes it possible to obtain beam profiles using EUV radiation and investigate the possibility of beam profile measurements
- We need to develop the strict model of EUV TR from different targets (material, shape, etc.)

THANK YOU FOR YOUR ATTENTION!